Boundary Feedback Control for Heat Exchange Enhancement in 2D Magnetohydrodynamic Channel Flow by Extremum Seeking

Lixiang Luo and Eugenio Schuster

***Abstract*— The heat exchange efficiency of electrically conducting fluids can drop dramatically when they interact with externally imposed magnetic fields. The movement of such fluids under the presence of imposed transverse magnetic fields can generate substantial magnetohydrodynamics (MHD) effects including the need of higher pressure gradients to drive the fluids and lower heat transfer rates due to the laminarization of the flows. Active boundary control can be employed to overcome this disadvantage. We consider in this work a heat exchange process in a 2D MHD channel flow. An extremum-seeking scheme is proposed to tune in real time a fixed-structure boundary controller with the ultimate goal of maximizing the outlet temperature of the electrically conducting cooling fluid, and therefore enhancing the efficiency of the heat exchanger. A heat transfer solver based on finite difference techniques is developed to predict the temperature dynamics within the 2D MHD channel, where the velocity dynamics is predicted by a pseudo-spectral solver. Simulation results show the efficiency of the proposed controller.**

I. Introduction

The heat transfer properties of electrically conducting viscous fluids moving in channels or ducts are an important subject of study in cooling systems within a strong electromagnetic environment. The interaction between electrically conducting fluids and magnetic fields in channel or duct flows generates significant magnetohydrodynamics (MHD) effects, which often result in lower heat transfer rates due to the laminarization of the flow. As an example, the possible usage of liquid metals or electrically conducting liquid salts as self-cooled blankets in magnetic confinement nuclear fusion reactors has been in consideration for many years. The main function of the coolant is the absorption of energy from the neutron flux generated by the fusion reaction and the transfer of heat to an external energy conversion system. In addition, if a breeder liquid metal such as liquid-lithium is considered, the blanket can also carry out the breeding of tritium, which is part of the fuel used by the reactor. The electrically conducting fluid flow is affected by the strong magnetic field used to confine the plasma inside the reactor. The MHD effects prevent present liquid-metal cooling systems from producing the heat transfer improvements which might be expected based on the much higher thermal conductivity and boiling point of the coolant. A good review of the research in this area can be found in [1].

Boundary control of fluid systems, implemented through micro electro-mechanical or electro-magnetic actuators and sensors, can be used to counteract the unfavorable MHD effects. By introducing unsteadiness, boundary controllers have the potential of enhancing mixing and consequently the convection-driven heat exchange rate. Flow control has attracted much interest and dramatically advanced in recent years [2], [3], [4]. In particular, boundary control of MHD flows has been considered for many years [5], [6], [7], [8], [9], [10]. Research subjects range from strongly coupled MHD problems, like liquid metal and melted salt flows, to weakly coupled MHD problems, like salt water flows. Our prior work includes the development of a feedback control scheme for mixing enhancement in a 2D MHD flow [11]. Nevertheless, early research mostly focused on passive and open loop control, partly due to the complexity of the coupled MHD equations. Unfortunately the nonlinearities and uncertainties of the system usually limit the effectiveness of these open-loop controllers, which are not optimized with respect to the varying flow conditions. Our previous efforts in this field also include the development of a fixed-structure controller for mixing enhancement which is optimally tuned via extremum-seeking [12]. The addition of heat transfer analysis further adds to the complexity and the work carried out on direct enhancement of heat transfer is limited.

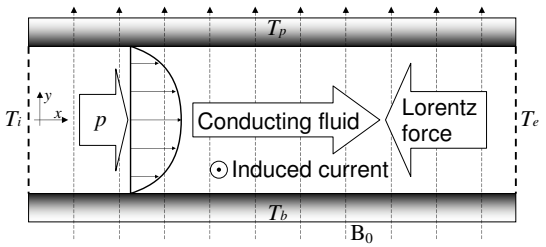

Fig. 1. 2D MHD flow between plates.

We consider in this work the simplified setting shown in Fig. 1. An electrically conducting fluid with inlet temperature T_i flows under the presence of an imposed transverse magnetic field B_0 through a section of a 2D channel with high-temperature walls (T_p and T_b), and eventually leaves this section with a higher outlet temperature T_e after absorbing internal energy from the walls. This setting can be seen as the idealization of a heat exchanger within an electromagnetic environment where an electrically conducting fluid such as a liquid metal is pumped through pipes with the goal of removing heat from the surrounding cooling blanket.

Using the outlet heat flux as a to-be-maximized cost function,we employ extremum seeking to optimally tune in real time a traveling-wave-like boundary controller in order to maximize the heat exchange rate in the considered MHD channel flow. Extremum seeking [13] is a very effective ap-

This work is supported by the NSF CAREER award program (ECCS–0645086). Lixiang Luo (lixiang.luo@lehigh.edu) and Eugenio Schuster (schuster@lehigh.edu) are with the Department of Mechanical Engineering and Mechanics, Lehigh University, Bethlehem, PA 18015, USA.

proach to build real-time feedback controllers based on fixed-structure control laws with tunable parameters [14], [15]. It is applicable in situations where there is a nonlinearity in the control problem, and the nonlinearity has a local minimum or a maximum. In addition, due to its non-model-based nature, extremum seeking is well suited to overcome the limitations described above in terms of uncertainty handling and is capable of capturing the input-output information of the otherwise highly complicated relationship between the control parameters and the heat exchange rate. However, simulations show that this relationship is highly nonlinear and sometimes nearly discontinuous, despite an overall trend can be clearly observed. This poses a serious challenge for extremum seeking, which essentially needs to recover gradient information from the probing signal. Previous work has confirmed that under this circumstances the optimization problem may not be well-posed [16]. Special measures are taken to overcome this difficulty, so that the overall trend of the cost function can be captured regardless of the occasional discontinuities.

This article is organized as follows. In Section II, we state the simplified MHD equations for incompressible MHD flows and present the associated heat exchange problem. In Section III, the feedback control scheme is discussed, including a brief introduction to extremum seeking. In Section IV, simulation results are presented for the proposed control scheme in a typical magnetohydrodynamic physical setting. The complex relation between the cost function and the to-be-optimized parameters is addressed. Section V closes the paper stating conclusions and identified future work.

II. Problem Statement

We consider a 2D, incompressible, electrically conducting fluid flowing between two parallel plates ($0<x<d=4\pi$, and $-1<y<1$) along the x-direction, as illustrated in Fig. 1, where an external magnetic field B_0 is imposed perpendicularly to the plates, i.e., in the y-direction. This flow was first investigated experimentally and theoretically by Hartmann [17]. The mass flux Q is fixed. A uniform pressure gradient P_x in the x-direction is required to balance the boundary drag force and the body force due to the MHD effects. Space variables x^* and y^*, time t^*, velocity field $\mathbf{v}^*$ are converted to their dimensionless forms: $x=\frac{x^*}{L}$, $y=\frac{y^*}{L}$, $t=\frac{t^*U_0}{L}$, $\mathbf{v}=\frac{\mathbf{v}^*}{U_0}$, where L and U_0 are the dimensional reference length and velocity. The velocity field is defined as $\mathbf{v}(x,y,t)=U(x,y,t)\hat{\mathbf{x}}+V(x,y,t)\hat{\mathbf{y}}$, where $\hat{\mathbf{x}}$ and $\hat{\mathbf{y}}$ are unit vectors on the x and y directions.

The characteristic numbers appearing in the system equations, including Reynolds number (inertia/viscosity forces), magnetic Reynolds number (magnetic advection/diffusion), Stuart number (magnetic/inertia forces) and Péclet number (thermal advection/diffusion), are defined as: $\mathrm{Re}=\frac{U_0L}{\nu}$, $\mathrm{Re_m}=\mu\sigma U_0L$, $\mathrm{N}=\frac{\sigma LB_0^2}{\rho U_0}$, $\mathrm{Pe}=\frac{\rho c_p U_0 L}{\lambda}$. The physical properties of the fluid, including the mass density ρ, the dynamic viscosity ν, the electrical conductivity σ, the magnetic permeability μ, the specific heat c_p, and the thermal conductivity λ, are all assumed constant.

In this paper, we consider MHD flows at low magnetic Reynolds numbers, which are also called simplified MHD (SMHD) flows. Under the assumption $\mathrm{Re_m}\ll 1$, the induced magnetic field is very small when compared with the imposed magnetic field B_0, and therefore negligible. The dynamics of the velocity field in a 2D SMHD channel flow is described by slightly modified incompressible N-S equations:

$$\frac{\partial \mathbf{v}}{\partial t}=\frac{1}{\mathrm{Re}}\nabla^2\mathbf{v}-(\mathbf{v}\cdot\nabla)\mathbf{v}+\nabla P+\mathrm{N}(\bar{U}-U)\hat{\mathbf{x}}, \tag{1}$$

$$\nabla\cdot\mathbf{v}=0, \tag{2}$$

where $\bar{U}$ represents the average speed, defined as $\bar{U}=Q/L$. More details on this simplified model can be found in [18]. The validity of using the simplified MHD model has been verified by many pieces of work [19]. In most engineering applications, the conditions $\mathrm{Re}\gg 1$ and $\mathrm{Re_m}\ll 1$ hold. Numerical simulations also confirm that under such physical settings, full MHD and SMHD give near identical results, while the former methods has to use much smaller time steps (characterized by CFL$\ll$1 [20]) than the latter method to ensure convergence [21]. The dynamics of the temperature field is described by the heat transfer equation

$$\frac{\partial T}{\partial t}=\frac{1}{\mathrm{Pe}}\nabla^2T+(\mathbf{v}\cdot\nabla)T. \tag{3}$$

The bottom and top walls are assumed non-slip. Hence, the velocity boundary conditions for the SMHD system are given by

$$U(x,\pm1,t)=0, \qquad V(x,\pm1,t)=V_{ctrl},$$

where V_{ctrl} is determined by the proposed boundary control laws. In the uncontrolled cases, $V_{ctrl}=0$. We assume periodic boundary conditions in the streamwise direction. In this work we consider a heat transfer process where the heat is removed from the system through the walls of the channel by a running fluid, which gives the boundary conditions as follows:

$$T(0,y,t)=T_0, \qquad \frac{\partial T}{\partial x}(d,y,t)=0,$$
$$T(x,\pm1,t)=T_0+T_d\left(1-e^{-x}\right).$$

For simulation purposes, the temperature distribution on the two walls are defined to roughly emulate the gradual heating of the fluid, while not introducing much discontinuity near the two inlet-wall corners.

At the two walls the heat flux is driven by conduction:

$$I_b=-\frac{1}{\mathrm{Pe}}\int_0^L\left.\frac{\partial T}{\partial y}\right|_{y=-1}dx, \qquad I_p=\frac{1}{\mathrm{Pe}}\int_0^L\left.\frac{\partial T}{\partial y}\right|_{y=1}dx.$$

The Dirichlet boundary condition at the inlet allows conduction-driven heat transfer. However, for the case studies in this work the heat transfer is assumed dominated by advection. According to the Neumann boundary condition at the outlet, heat transfer is driven exclusively by advection. Therefore,

$$I_e=\int_{-1}^{1}(vT)|_{x=L}\,dy, \qquad I_i=T_i\int_{-1}^{1}v|_{x=0}\,dy=QT_i.$$

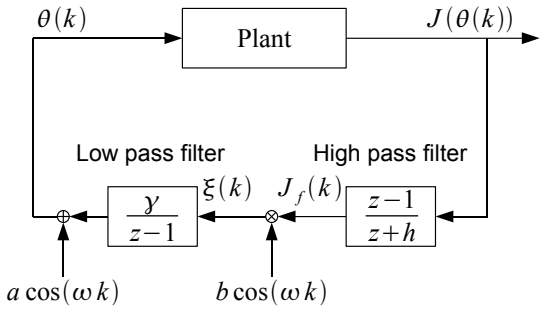

Fig. 2. Extremum seeking control scheme. The variable z denotes the Z-transform variable, h and γ are constants specifying the filters, ω denotes the frequency of the probing signals, a and b are the amplitudes of the sinusoidal signals.

The integrated heat flux balance $\int_{t_0}^{t_0+t_i} I_i + I_b + I_p - I_e dt$ should remain zero for long enough t_i. This serves as a basic consistency criterion for the heat transfer solver. Simulation results for stable flows agree very well with this equation, while turbulent flows may show slight disagreement.

III. Extremum Seeking Feedback Control

We propose a fixed-structure control law given by a traveling wave as the boundary condition,

$$V(x,\pm 1,t) = V_{ctrl} = A\sin(kx+\theta t), \tag{4}$$

where the constant A is the maximum amplitude, k is the wave number, and θ is the angular frequency, which is also called the phase speed in this work.

The performance of this fixed-structure control law is largely determined by k and θ, which control the frequency and moving speed of the control "wave". For the controller to excite the vortices, this "wave" needs to be in synchronization with the corresponding major unstable mode. Assuming that the average speed of the vortices is V_e, the number of vortices on one side is N_e, which is half of the total number of vortices since they appear in pairs on two sides, and the total number of periods of the control "wave" is N_c, we can determine that the fixed-structure control law should fulfill the condition $N_c = N_e$ and $\theta = V_e$ in order to excite the major unstable mode. In the case of the parameter k, the optimal value is an integer related to the number of major vortices. In this work, we find that $k=1$ is usually the optimal choice as it produces the same number of major vortices as most fully developed flows do (see Fig. 5 for a typical flow pattern). However, the value of θ is more difficult to determine because it is not an integer. Extremum seeking has been proved effective for a wide range of linear and nonlinear optimization problems, making itself an ideal candidate for optimally tuning in real time the value of θ in order to maximize a functional related to heat transfer.

The extremum seeking scheme is illustrated in Fig. 2 as a block diagram. At each iteration step, the flow is let evolve with a traveling wave of phase speed $\theta(k)$ as boundary condition. The phase speed $\theta(k)$ contains a superimposed sinusoidal perturbation (modulation). A cost function J related to heat transfer is evaluated using the response of the system to the phase speed $\theta(k)$. The cost function signal is

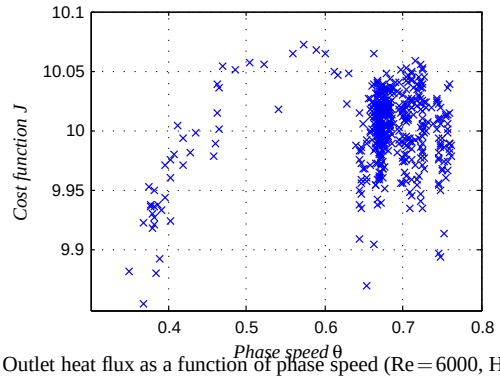

Fig. 3. Outlet heat flux as a function of phase speed (Re = 6000, Ha = 1.04).

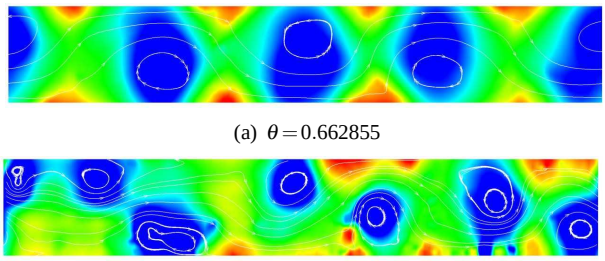

(a) $\theta = 0.662855$

(b) $\theta = 0.663060$

Fig. 4. Pressure maps and streamlines for two very close phase speeds.

then filtered by a high-pass filter and multiplied by another sinusoidal signal of identical frequency (demodulation). The demodulated signal ξ, containing gradient information of the system, is filtered through a low-pass filter and used to generate an updated phase speed $\theta(k+1)$ to be used during the next iteration step. Detailed explanation of this scheme can be found in [13].

The to-be-minimized cost function J is defined in this work as a time-averaged version of the outlet heat advection I_e. This cost function measures the amount of internal energy being carried downstream by the flow, which is proportional to the amount of energy being transferred from the hot walls to the cooler fluid. Snapshots of I_e values are taken every 20 simulation steps and the standard deviation of the collected data is calculated using the last 200 samples. Once this standard deviation decreases below a specific threshold, we consider the flow statistically steady and the system output J is computed by integrating I_e over the same period of time used for the standard deviation calculation.

Extremum seeking is very effective in optimizing systems with cost functions that are continuous and with a well-defined extremum. However, extremum seeking may not capture the gradient information and fail if the cost function is not smooth or even discontinuous. Such situation does arise in our work, as the cost function has many sudden changes near the optimal point. The complexity of the cost function is shown in Fig. 3, where the time-averaged outlet heat flux is plotted as a function of the phase speed θ. Although a clear trend can be noticed in the figure, the cost function seems extremely sensitive to phase speed changes, especially near the optimal point around 0.6. Let us take, for instance, two data points in Fig. 3. The steady state value for I_e drops from 10.0638 to 9.9045 when the phase

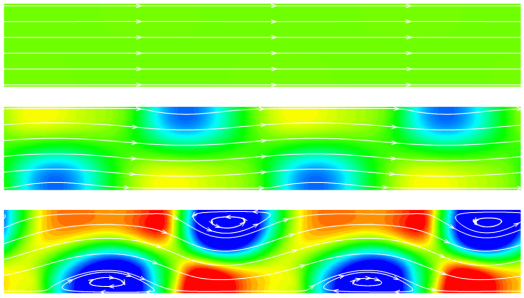

Fig. 5. Pressure maps and streamlines for Re = 7500 (t =266, 1590, 2973).

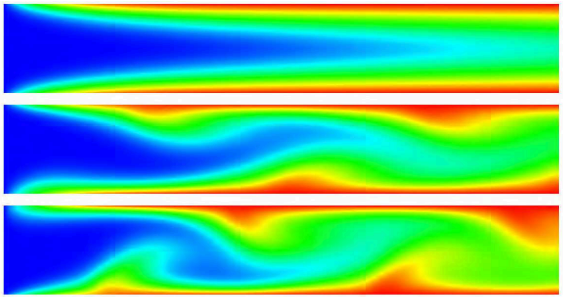

Fig. 6. Temperature maps for Re=7500 (t =266, 1590, 2973).

speed changes from 0.662855 to 0.663060. Considering that the overall range for J goes from 8.9 (laminar flows) to no more than 10.1, this sudden drop of cost function can cause significant challenges during the optimization. The difference of flow patterns can be clearly seen from the pressure maps and stream lines in Fig. 4. While the case with higher I_e has four sustaining organized vortices, the case with smaller I_e has seven smaller deformed vortices. However, the boundary control "wave" has only two full periods in the streamwise direction. As a result, the vortices cannot be well excited by the boundary control because of the lack of synchronization.

This discontinuous behavior is largely caused by the nonlinearity of the flow. To enhance heat exchange, the boundary control needs to produce large sustaining vortices in the flow to enhance mixing. Due to its nonlinearity nature, the development of vortices is seriously affected by the initial conditions and random numerical noise. It may take extensive long time for the flow to reach the statistically steady state. Furthermore, a flow with specific physical settings may have more than one statistically steady state and may not converge to the one with highest cost function value.

To counteract the unfavorable effects of the discontinuity of the cost function, special techniques are implemented within the extremum seeking algorithm. First, the perturbation signal $a\cos(\omega k)$ is reduced in the region with significant discontinuity in order to reduce the possibility of sudden big changes in the cost function value. Second, a low-pass filter is added immediately after the plant output. This filter provides the average of the most recent 5 plant outputs $J(\theta(k))$ (including the latest plant output). Theis averaging technique can eliminate most of the discontinuity while capturing the overall trend, thus increasing the ability of the extremum seeking to stay inside the optimal region.

IV. Simulation Results

The velocity-field numerical simulations are carried out by a modified Navier-Stokes solver. The equations are discretized using FFT on the streamwise direction and finite differences on the spanwise direction, which is also called the pseudospectral method. Time integration is done using a fractional step method along with a hybrid Runge-Kutta/Crank-Nicolson scheme. Linear terms are treated implicitly by the Crank-Nicolson method and nonlinear terms are treated explicitly by the Runge-Kutta method. The divergence-free condition is fulfilled by the fractional step method.

A separate heat transfer solver is used to simulate the temperature-field evolution. Due to the limitations of pseudospectral method for imposing boundary conditions at the channel inlet and outlet, a finite difference method is employed to solve the heat exchange problem. The grid is identical to the one used for the velocity-field pseudospectral method. The temperature is defined at the same locations where the streamwise component of the velocity field is defined. The heat transfer equation is linear, given the fact that the velocity field is solved separately and known when the temperature field is solved. This enables implicit time integration of the heat transfer equation, which is carried out in this work by the Crank-Nicolson method. To ensure physical consistency for the heat transfer equation, an upwind scheme is necessary. Otherwise, meaningless spots hotter than T_0+T_d or colder than T_0 will appear. The Alternating Direction Implicit (ADI) method is used to avoid solving a large-scale sparse linear system. For more details on the implementation of these techniques, see [20].

All the simulations are carried out for the same flow domain: $-1<y<1$, $0<x<4\pi$. The same mesh is used in all the simulations presented in this section (grid points in the x direction: NX = 150, grid points in the y direction: NY = 128). We consider $T_0=5$ and $T_d=2$ in all cases. Similarly, we adopt $Q=1.5$.

A. MHD flows with no control

When $B_0=0$, the momentum equation (1) reduces to the standard incompressible Navier-Stokes equation characterizing the well-known Poiseuille flow. Poiseuille flows in 2D channels can be linearly stable for low Reynolds numbers, as infinitesimal perturbations in the flow field are damped out. The flows turn linearly unstable for high Reynolds numbers Re$>$5772 [22], [23]. Such flows usually reach statistically steady states, which we call fully established flows. Fig. 5 show how a channel flow (Re=7500) develops to a fully established flow. The pressure maps and streamlines, given by Fig. 5, illustrate how the vortices evolves in time until reaching a fully established flow when the initial equilibrium velocity profile is infinitesimally perturbed at $t=0$.

The flow pattern inside the channel has a major influence on heat exchange. The temperature maps in Fig. 6 closely resemble the flow pattern already seen in Fig. 5. As shown in Fig. 7, the large vortices significantly increase the heat transfer rate I_b and I_p at the walls. Since the heat inflow I_i is constant, and the overall heat flux must be balanced, the heat

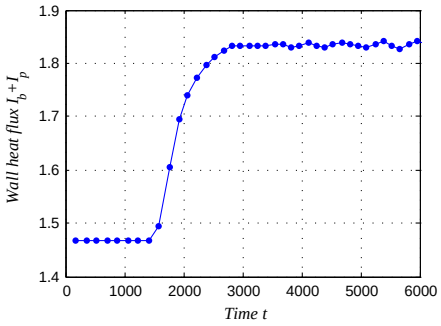

Fig. 7. Heat flux at the walls (Re = 7500).

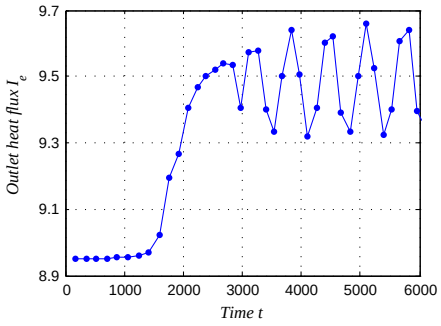

Fig. 8. Heat flux at the outlet (Re = 7500).

outflow I_e must increase, as shown in Fig. 8. The temperature maps in Fig.6 provide an intuitive explanation of the heat transfer process. Because of the vortices, the region with lower temperature stretches closer to the walls, resulting in a larger temperature gradient and a higher heat transfer rate. The span of the colder region in the streamwise direction becomes shorter as the vortices develop, increasing the overall outlet temperature and consequently the advection-driven heat transfer rate.

When $B_0 \neq 0$, Fig. 9(a) shows the heat flux for different Hartmann numbers $\mathrm{Ha} = \sqrt{\mathrm{N} \cdot \mathrm{Re}}$. The enstrophy is commonly used to quantify the overall turbulence of the velocity field. In our work we use the averaged enstrophy, defined by

$$E_s = \frac{1}{2d} \int_{-1}^{1} \int_{0}^{d} \frac{1}{2} \left(\frac{\partial v}{\partial x} - \frac{\partial u}{\partial y} \right)^2 dxdy. \tag{5}$$

As shown in Fig. 9(a), the enstrophy decreases as the flow is stabilized by the imposed magnetic field. The simulation is started at $t = 0$ with the fully established flow achieved in Fig. 5. We can see that stronger imposed magnetic fields tend to make the flow more stable. By comparing Fig. 9(a) with Fig. 9(b) and Fig. 9(c), showing the heat flux both at the walls and the outlet for different Hartmann numbers, we can note that the wall heat flux and the enstrophy are highly correlated. For $\mathrm{Ha} = 1.83$, the heat flux is reduced to a very low level because vortices are completely suppressed.

B. MHD flows with extremum-seeking feedback control

The simulations start with the equilibrium solutions achieved after the external magnetic fields are imposed. These flows remain linearly stable indefinitely if no boundary control is present. The optimal extremum-seeking controller is expected to drive these flows to states with better outlet heat exchange rate I_e. Simulations are conducted for Case 1: $\mathrm{Re} = 6000$, $\mathrm{Ha} = 1.04$ and Case 2: $\mathrm{Re} = 7500$, $\mathrm{Ha} = 1.83$. The initial phase speed is set to 0.35 for both simulation cases. The parameters for extremum seeking have to be carefully chosen to balance the stability and performance of the optimization process. In this case, we use $a = 0.004$ for $\theta < 0.5$ and $a = 0.002$ for $0.5 < \theta < 0.9$, $\omega = 3$, $\gamma = 0.3$, $h = 0.8$ (see Fig. 2), $A = 0.05$, $k = 1$ (see (4)).

As we can see in Fig. 10(a), the boundary control based on extremum seeking gradually adjusts the phase speed in order to maximize the heat-transfer-related cost function. Even though the controller cannot keep the system at the optimal phase speed all the time, it manages to stabilize the phase speed near the optimum, regardless of significant amount of randomness in the cost function.

As illustrated in Fig. 10(b), the increase of enstrophy by several times indicates that unsteadiness is greatly enhanced by our proposed control scheme. Let us focus on Case 2. From Fig. 8 we can see that in a fully laminar flow the heat exchange rate at the outlet is around 8.95 (indicated as "Stable flow" in Fig. 10(c)), while in a fully developed flow the heat exchange rate at the outlet is around 9.5, implying that the vortices in the fully developed flow produce an increase of 0.55 in the heat exchange rate. However, an imposed magnetic field with moderate strength ($\mathrm{Ha} = 1.83$) can completely laminarize the flow as shown in Fig. 9(a) and reduce the heat exchange rate back to 8.95 as shown in Fig. 9(c). As we can note from Fig. 10(c), the extremum seeking controller succeeds in increasing the heat exchange rate at the outlet from 8.95 for the flow stabilized by the imposed magnetic field to 10.05, which is even higher than the 9.5 value achieved by the fully developed flow when no magnetic field is present. The effect of the enhanced unsteadiness on the heat exchange rate can be clearly seen in the temperature maps shown in Fig. 11. Due to the large sustaining vortices, the cool fluid from the inlet quickly mixes with the hot fluid near the walls, effectively increasing the heat transfer between the fluid and the walls.

V. Conclusion

A boundary feedback control scheme based on a fixed-structure controlled optimally tuned by extremum seeking has been proposed for heat exchange enhancement in a 2D MHD channel flow. Simulation results show that the control scheme successfully destabilize the otherwise linearly stable flow, increasing the heat exchange rate between the fluid and the channel walls. As a consequence, the fluid temperature at the channel outlet is significantly increased, maximizing in this way heat extraction. The extremum seeking method can effectively optimize the parameter of the fixed-based controller by maximizing a system output whose relationship with the optimized parameter would be extremely hard to model. The tuning of the extremum seeking scheme is crucial for the success of the control scheme. A simple but effective method based on averaging is used to avoid disruptions caused by cost function discontinuities during the extremum-seeking optimization process. Extension to 3D MHD flows and design of more robust methods to deal with the cost-function discontinuities are part of our future work.

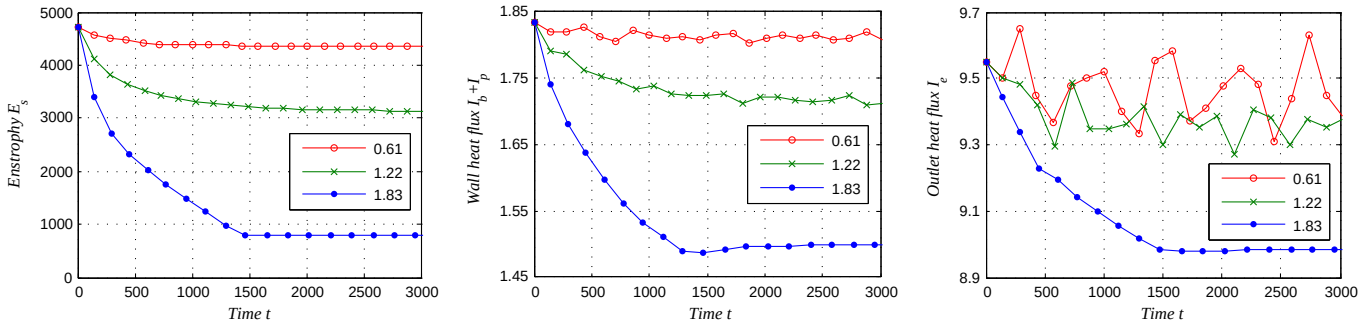

(a) Enstrophy (b) Wall heat flux (c) Outlet heat flux

Fig. 9. MHD flows with different Hartmann numbers.

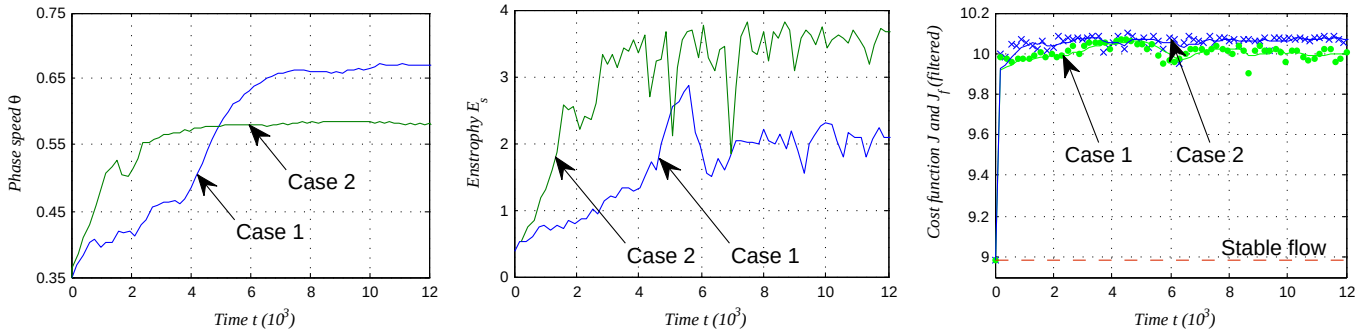

(a) Phase speed (b) Enstrophy (c) Cost function (lines: J, points: J_f)

Fig. 10. Extremum-seeking-controlled MHD flows.

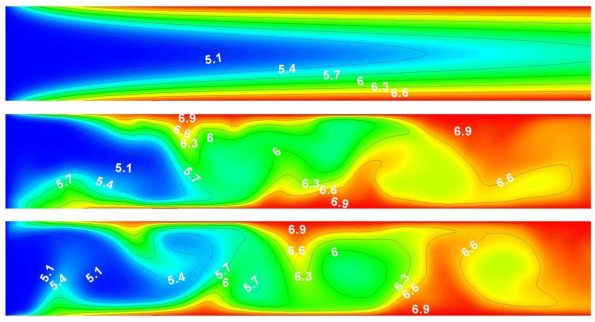

Fig. 11. Temperature map (Case 1, t=0,2500,14097).

REFERENCES

[1] U. Müller and L. Bühler, *Magnetofluiddynamics in channels and containers*. Springer, 2001.

[2] M. D. Gunzburger, *Flow Control*, ser. The IMA Volumes in Mathematics and its Applications. New York: Springer-Verlag, 1995, vol. 68.

[3] S. S. Sritharan, Ed., *Optimal control of viscous flow*. SIAM, Philadelphia, 1998.

[4] O. M. Aamo and Krstić, *Flow Control by Feedback*. Springer, 2002.

[5] A. B. Tsinober, *Viscous Drag Reduction in Boundary Layers*, ser. Progress in Astronautics and Aeronautics. Washington, DC: AIAA, 1990, no. 123, ch. MHD flow drag reduction, pp. 327–349.

[6] C. Henoch and J. Stace, "Experimental investigation of a salt water turbulent boundary layer modified by an applied streamwise magnetohydrodynamic body force," *Physics of Fluids*, vol. 7, no. 6, pp. 1371–1383, June 1995 1995.

[7] H. Choi, D. Lee, and J. Lim, "Control of near-wall streamwise vortices using an electromagnetic force in a conducting fluid," *AIAA Paper*, vol. 97-2059, 1997.

[8] T. Berger, J. Kim, C. Lee, and J. Lim, "Turbulent boundary layer control utilizing the Lorentz force," *Physics of Fluids*, vol. 12, p. 631, 2000.

[9] E. Spong, J. Reizes, and E. Leonardi, "Efficiency improvements of electromagnetic flow control," *Heat and Fluid Flow*, vol. 26, pp. 635–655, 2005.

[10] R. Vazquez and M. Krstic, *Control of Turbulent and Magnetohydrodynamic Channel Flows: Boundary Stabilization and State Estimation*. Birkhäuser Boston, 2007.

[11] E. Schuster, L. Luo, and M. Krstic, "MHD channel flow control in 2d: Mixing enhancement by boundary feedback," *Automatica*, vol. 44, no. 10, pp. 2498 – 2507, 2008.

[12] L. Luo and E. Schuster, "Mixing Enhancement in 2D Magnetohydrodynamic Channel Flow by Extremum Seeking Boundary Control," *Proceedings of the 2009 American Control Conference*, June 10-12, 2009 St. Louis, Missouri, USA.

[13] K. Ariyur and M. Krstić, *Real-time optimization by extremum-seeking Control*. Wiley-Interscience, 2003.

[14] J. Beaudoin, O. Cadot, J. Aider, and J. Wesfreid, "Bluff-body drag reduction by extremum-seeking control," *Journal of Fluids and Structures*, vol. 22, no. 6-7, pp. 973–978, 2006.

[15] R. King, R. Becker, G. Feuerbach, L. Henning, R. Petz, W. Nitsche, O. Lemke, and W. Neise, "Adaptive flow control using slope seeking," *Proceedings of 14th Mediterranean Conference on Control and Automation*, pp. 1–6, June 2006.

[16] B. Protas, T. Bewley, and G. Hagen, "Some formulation issues in adjoint-based optimal estimation and control of PDEs," (preprint).

[17] J. Hartmann, *Theory of the laminar flow of an electrically conductive liquid in a homogeneous magnetic field*, xv(6) ed. Det Kgl. Danske Vidensk-abernes Selskab. Mathematisk-fysiske Meddelelser.

[18] G. Branover, *Magnetohydrodynamic flow in ducts*. Halsted Press, 1979.

[19] D. Lee and H. Choi, "Magnetohydrodynamic turbulent flow in a channel at low magnetic reynolds number," *Journal of Fluid Mechanics*, vol. 439, pp. 367–394, 2001.

[20] J. Anderson, *Computational fluid dynamics, the basics with applications*. McGraw-Hill, 1995, pp. 153–165.

[21] H. Choi and P. Moin, "Effects of the computational time step on numerical solutions of turbulent flow," *Journal of Computational Physics*, vol. 113, no. 1, pp. 1–4, 1994.

[22] R. L. Panton, *Incompressible flow*, 2nd ed. New York: Wiley, 1996.

[23] P. J. Schmid and D. S. Henningson, *Stability and transition in shear flows*. New York: Springer, 2001, vol. 142.